Temperature-dependent optical band gap of the metastable zinc-blende structure β-GaN

G. Ramírez-Flores, H. Navarro-Contreras, and A. Lastras-Martínez
Instituto de Investigación en Comunicación Optica, Universidad Autónoma de San Luis Potosí, 78000 San Luis Potosí, SLP, México

R. C. Powell* and J. E. Greene
Materials Science Department, Coordinated Science Laboratory, and Materials Research Laboratory, University of Illinois, 1101 West Springfield Avenue, Urbana, Illinois 61801

(Received 21 March 1994)

The temperature-dependent (10–300 K) optical band gap $E_0(T)$ of the epitaxial metastable zinc-blende-structure β-GaN(001)4×1 has been determined by modulated photoreflectance and used to interpret low-temperature photoluminescence spectra. E_0 in β-GaN was found to vary from 3.302±0.004 eV at 10 K to 3.231±0.008 eV at 300 K with a temperature dependence given by $E_0(T) = 3.302 - 6.697\times10^{-4}T^2/(T+600)$ eV. The spin-orbit splitting Δ_0 in the valence band was determined to be 17±1 meV. The oscillations in the photoreflectance spectra were very sharp with a broadening parameter Γ of only 10 meV at 10 K. The dominant transition observed in temperature-dependent photoluminescence was attributed to radiative recombination between a shallow donor, at ≅11 meV below the conduction-band edge and the valence band.

I. INTRODUCTION

α-GaN is a refractory III-V semiconductor with a hexagonal wurtzite equilibrium crystal structure and a large direct band gap, 3.4 eV at 300 K. Interest in the growth and physical properties of GaN stems primarily from the desire to utilize this material to fabricate a variety of near-UV optoelectronic devices including blue-light-emitting diodes.[1] GaN is also predicted to have a high ballistic-electron drift velocity.[2] However, the success of GaN optoelectronic devices has been limited due to the presence of large intrinsic donor concentrations—typical films have high concentrations ($\geq 10^{18}$ cm^{-3}) of shallow donors attributed to N vacancies—and the lack of high-quality lattice-matched substrates. α-GaN is usually grown on Al_2O_3 (0001) with which it has a lattice-constant mismatch of ≅16%. Recently, it has been demonstrated that epitaxial metastable zinc-blende structure β-GaN, with a lattice constant of 0.4530 nm,[3] can be grown pseudomorphically on cubic substrates such as MgO(1×1).[3,4] Although still lattice-constant mismatched, ≅7%, the possibility of growing the cubic phase increases the number of available substrates and epitaxial β-GaN has been deposited on the (001) surface of GaAs,[5,6] β-SiC,[7,8] and Si.[9]

Empirical and model pseudopotential band-structure calculations for β-GaN (Refs. 10–12) have predicted a room-temperature direct band gap, which is ≅0.1–0.6 eV less than that of α-GaN. There is, however, considerable disagreement among experimental results. Most of the measurements have been carried out with films on optically opaque substrates using cathodoluminescence (CL). Okumura, Misawa, and Yoshida[13] observed a single broad CL emission feature ($h\nu \cong 3.81$ eV) at 77 K from β-GaN grown on GaAs. Strite *et al.*[6] measured the CL spectra as a function of temperature from β-GaN grown on GaAs and found several groups of emission peaks. They assumed that the highest energy emission, though weak, was due to band-to-band recombination in β-GaN and estimated that E_0 varied from ≅3.52 eV at 4 K to ≅3.45 eV at room temperature. However, a stronger set of emissions, presumed to be due to free-electron-bound hole and donor-acceptor transitions, was observed at all temperatures, and, at 280 K, consisted of a single peak at 3.206 eV. Davis[14] reported the band gap of β-GaN on β-SiC to be 3.26 eV but provided no information as to how the measurement was made. Recently, Powell *et al.*[3] obtained a value of E_0 (300 K)=3.21 ±0.02 eV from transmission and/or reflection measurements carried out on β-GaN films grown on MgO.

In this article, we present the results of an investigation using modulated photoreflectance, together with photoluminescence, to determine both the direct optical band gap E_0 and the valence-band spin-orbit splitting Δ_0 for metastable zinc-blende structure β-GaN as a function of temperature between 10 and 300 K.

II. EXPERIMENTAL PROCEDURE

All β-GaN films examined were grown on MgO(1×1) substrates by reactive-ion molecular-beam epitaxy (RIMBE) in which the primary source of nitrogen is a low-energy (35 eV) N_2^+ ion beam extracted from an ultrahigh vacuum hot-cathode single-grid source with magnetic confinement. The incident N_2^+ to thermal Ga ratio at the substrate was 2.0 with a film growth temperature of 650 °C. A detailed description of the growth procedure has been published elsewhere.[3] The films analyzed ranged in thickness from 1–1.5 μm and were shown by *in situ* reflection high-energy electron diffraction (RHEED) and post-deposition double-crystal x-ray diffraction, plane-view transmission electron diffraction (TEM), and cross-sectional TEM (XTEM) to be epitaxial with a 90°-rotated two-domain (4×1) surface reconstruction. The

0163-1829/94/50(12)/8433(6)/$06.00 ©1994 The American Physical Society

films are n-type as discussed in detail in Ref. 3 due, presumably, to N vacancies as in α-GaN. Typical electron concentrations in the films used in this work were $\geq 10^{18}$ cm^{-3}. Substrate preparation basically consists of degreasing commercially polished MgO(001) in successive rinses of trichloroethane, acetone, methanol, and isopropyl alcohol. The samples were then blown dry in dry N_2, loaded into the growth chamber, and heated to 800 °C for 2 min. This procedure yields strong (1×1) RHEED and low-energy-electron-diffraction patterns with sharp Kikuchi lines.[3] Photoreflectance (PR) measurements were carried out on specimens cut from the edge of as-deposited layers in order to maximize the variation in film thickness across the samples and hence to minimize the effect of interference fringes in the optical spectra.

Figure 1(a) schematically illustrates the experimental arrangement for the PR measurements. Light from a Xe lamp was dispersed through a 0.5-m focal length monochromator and intersected the sample at an angle $\cong 5°$ to the sample normal. The optical modulation was provided by the 325-nm line of a 10-mW He-Cd UV laser beam mechanically chopped at a frequency $f = 100$ Hz and incident at an angle of 30°. An interference filter with a pass-band centered at 325 nm was used to eliminate parasitic plasma emissions from the UV laser while a long-wavelength bandpass filter prevented scattered radiation from reaching the detectors. Specularly reflected light was detected using a Si diode, whose signal was fed into a lock-in amplifier tuned to 100 Hz. The signal was then processed by a microscomputer to obtain $\Delta R/R$ as a function of incoming photon energy. R is the reflectivity in the absence of the laser light and ΔR is the absolute difference in reflectivity with and without UV laser exposure.

The chopped laser beam was also used as the excitation source during the photoluminescence (PL) measurements, as shown in Fig. 1(b), and the emitted light dispersed through the 0.5-μm monochromator. The PL signal was detected with a UV-enhanced photomultiplier, cooled to -30 °C. Temperature-dependent PR and PL measurements were carried out by mounting the samples on the cold finger of a closed-cycle He refrigerator with quartz optical windows. The sample temperature was measured to an accuracy of ± 0.25 K and calibrated with a chromel/AuFe thermocouple. The samples were mounted on the cold finger so that they could contract freely as the temperature is lowered in order to avoid external strain effects.

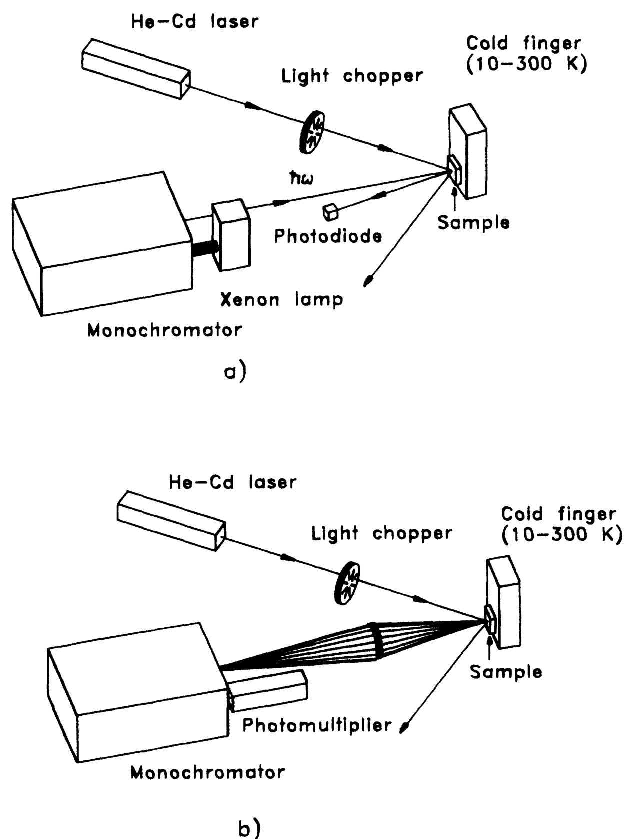

FIG. 1. Schematic diagrams of the experimental arrangements and optical paths for the (a) modulated photoreflectance and (b) photoluminescence measurements.

III. EXPERIMENTAL RESULTS AND DISCUSSION

Figure 2 shows typical modulated photoreflectance $\Delta R/R$ spectra plotted as a function of incident photon energy E for sample temperatures between 10 and 300 K. $\Delta R/R$ is the normalized change in the photoreflectance due to the modulation of the surface electric field by the photoinjected charge carriers.[15] The overall shape of the spectra in Fig. 2 is similar to that obtained from other single-crystal semiconductors such as GaAs (Ref. 16) exhibiting a double oscillation due to transitions at two critical points in the reduced Brillouin zone. The lower-energy feature corresponds to the direct optical band gap E_0, while the higher-energy features at $E_0+\Delta_0$ is due to

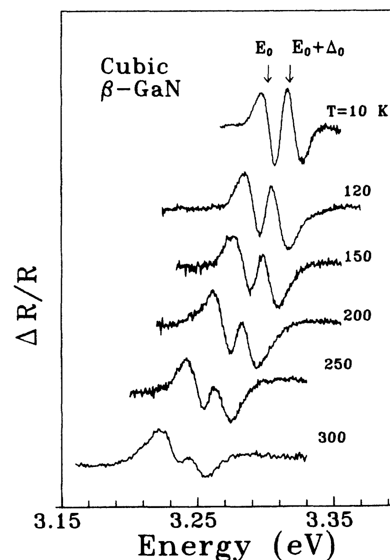

FIG. 2. Typical modulated photoreflectance $\Delta R/R$ from zinc-blende structure β-GaN as a function of incident photon energy E at temperatures between 10 and 300 K.

the addition of the spin-orbit-splitting energy in the valence band. The very narrow energy width of the oscillations in Fig. 2, comparable to modulated electroreflectance data from GaAs obtained at 4.2 K,[16] is an indication of the relatively high quality of the epitaxial layers.

PR spectra are typically fit using the well-developed theory for modulated electroreflectance,[17] the essential features of which are discussed below. We assume in the fitting that the PR is due to two closely spaced, in energy, valence bands in β-GaN: The uppermost being a fourfold degenerate Γ_8 $J=\frac{3}{2}$ band and the lower a spin-orbit split Γ_7 $J=\frac{1}{2}$ band.[18] The experimentally observed function $\Delta R/R$ is related to the perturbation-induced changes in the complex dielectric function $\varepsilon=\varepsilon_1+i\varepsilon_2$ through the expression:[17]

$$\frac{\Delta R}{R}=\mathrm{Re}(Ce^{i\theta}\Delta\varepsilon)\ , \tag{1}$$

where C is the line-shape amplitude and θ is a phase angle, which depends upon the details of the model employed to describe the spectra. In the low-field limit, Aspnes[17] has demonstrated that the induced changes in the dielectric function are given by

$$\Delta\varepsilon=\frac{(\hbar\Omega)^3}{3E^2}\frac{\partial^3}{\partial E^3}[E^2\varepsilon(E)]\ , \tag{2}$$

where $\hbar\Omega$ is the electro-optical energy gained by photoexcited carriers due to band bending. Photoreflectance, like electroreflectance, is thus a third derivative technique and, hence, is very sensitive to band structure near critical points where there is a high joint density of states due to the conduction and valence bands being parallel.

The form of the dielectric function $\varepsilon(E)$ depends upon the dimension of the critical point, which is assigned according to the number of finite masses or curvature radii of the bands resulting from the energy difference E_c-E_v, where E_c and E_v are the conduction- and valence-band critical-point energies, respectively. For a three-dimensional M_0 critical point, i.e., for transitions to or from bands with isotropic parabolic masses,[17,18] the dielectric function can be written as[17]

$$\varepsilon(E,\Gamma)=\mathrm{B}i^{3/2}(E-E_g+i\Gamma)^{1/2}\ , \tag{3}$$

where Γ is the broadening parameter due to carrier scattering processes; B is a parameter that depends on the dipole moment matrix element, the energy, and the charge-carrier effective masses,[17] and $E_g=E_c-E_v$.

Expressions for the optical-modulation-induced changes in real $\Delta\varepsilon_1$ and imaginary parts $\Delta\varepsilon_2$ of the dielectric function can be obtained by substituting (3) into (2) and taking the third derivative. $\Delta\varepsilon$ is then substituted into Eq. (1), where C and θ are treated as fitting parameters. The low-field condition corresponding to Eq. (2) is not generally perfectly applicable. It has been shown for many semiconductors, including GaAs and Ge, that it is difficult to reach the low-field limit at energies near the direct gap.[16,19] (We estimate in the Appendix that the present experiments were carried out under conditions just above the low-field limit.) Nevertheless, as demonstrated by Aspnes and Rowe[19] the use of the low-field model to fit line shapes obtained in the high-field limit still yields the correct values for the transition energies. This is because the higher-field line shape is described by a combination of the same basic Lorentzian components used to describe the low-field line shape, the only difference being in the relative weighting factors. The latter is properly addressed by the inclusion of the phase angle θ.[19]

A typical fitted β-GaN $\Delta R/R$ spectra, in this case $T=10$ K, is shown in Fig. 3. The best fit was obtained using $\theta=1.21$ for the E_0 transition and 0.48 for the $E_0+\Delta_0$ transition, while the amplitude C was maintained constant. A measure of the degree of fit for this type of data is given by one minus the square root of the ratio of mean quadratic deviation of the fitted line shape, with respect to the experimental points, to the mean quadratic amplitude of the experimental spectrum. For Fig. 3, this yields a value of $\cong 0.9$. Equally good fits were obtained for measurements at 30 different temperatures throughout the range investigated, 10–300 K. The broadening parameter Γ was found to increase monotonically, as expected, with increasing temperatures, from $\cong 10$ meV at 10 K to $\cong 20$ meV at 300 K. In order to estimate the accuracy in the determination of the E_0 and $E_0+\Delta_0$, we allowed both the transition energies and the phase angles to vary around their optimum values. Maintaining the mean quadratic deviation within $\pm 10\%$ of the minimum value, the variation in the low-temperatures transition energies is within ± 2 meV. Including the precision of the experimental measurements, yields an overall uncertainty ranging between ± 0.004 eV at 10 K and ± 0.008 eV at 300 K.

Fitted values for the E_0 and $E_0+\Delta_0$ transition energies are shown as a function of temperature in Fig. 4. E_0 varies from 3.302 ± 0.004 eV at 10 K to 3.231 ± 0.008 eV at 300 K with a valence-band spin-orbit splitting of $\Delta_0=17\pm 1$ meV as estimated from the scattering of the

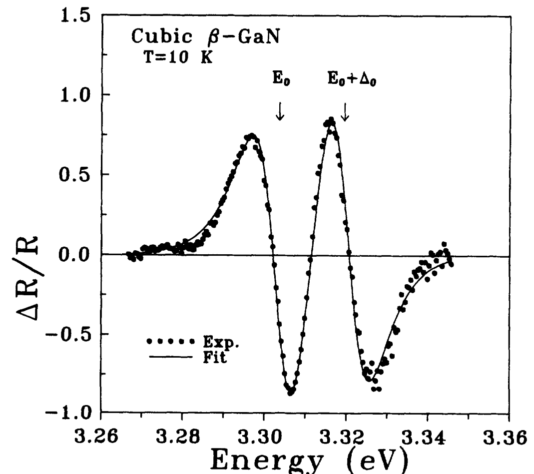

FIG. 3. Modulated photoreflectance spectra from zinc-blende structure β-GaN at 10 K fitted using Eqs. (1)–(3) to obtain the direct optical band gap E_0 and the spin-orbit splitting Δ_0 in the valence band.

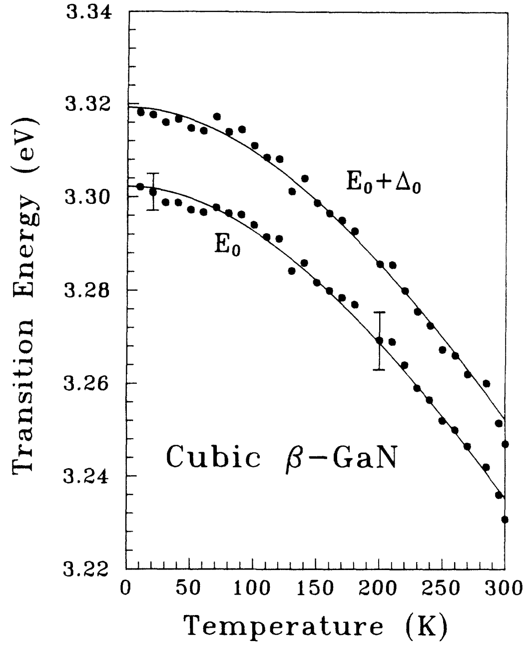

FIG. 4. Energies of the E_0 (lower curve) and $E_0+\Delta_0$ (upper curve) transitions in zinc-blende structure β-GaN at temperatures between 10 and 300 K.

whole set of experimental differences between those two transition energies. The solid lines in Fig. 4 are least-squares fits to the experimental data points using an empirical expression developed by Varshni[20] to describe the temperature dependence of the energy gaps of group-IV and III-V cubic semiconductors

$$E(T)=E(0)-\frac{AT^2}{T+\theta}\ , \tag{4}$$

where Θ is the Debye temperature and A is a fitting parameter. Since neither the Debye temperature nor the sound velocity for β-GaN are known, we used the Debye temperature for α-GaN, which has been estimated to be 600 K.[21] Figure 4 shows that the results are very well described by Eq. (4) with $A=6.697\times10^{-4}$ K^{-1} and $T=0$ K optical band gap $E_0(0)=3.302$ eV. The results are not strongly dependent upon the exact value of Θ used in the fitting. Similar quality fits are obtained by varying Θ between 600 and 1200 K. In the latter case, $E_0(0)$ increases to 3.303 eV, well within the uncertainty in the determination of $E_0(T)$. Moreover, our room-temperature result, E_0 (300 K)=3.231 eV, is in good agreement with the optical absorption measurements of Powell *et al.*[3] who obtained 3.21±0.02 eV while our fitted value for $E_0(0)$ is in good agreement with the theoretical estimate of Bloom *et al.*, 3.31 eV.[10] The higher values of E_0, which have been reported for β-GaN based upon cathodoluminescence measurements, E_0 (300 K)=3.45 eV (Ref. 6) and E_0(77 K)=3.81 eV,[13] we believe stem from inclusions of second-phase α-GaN grains in the films as discussed below.

The spin-orbit-splitting parameter Δ_0 we obtain for β-GaN, 17 meV, is consistent with the results for other cubic semiconductors for which Δ_0 is known. Plotting log(Δ_0) vs the lattice parameter a_0 for the III-V compounds GaP,[22] InP,[23] AlAs,[24] GaAs,[16] InAs,[25] GaSb,[26] AlSb,[27] InSb,[28] as well as the group-IV semiconductors Si,[29] Ge,[30] α-Sn,[31] and CSi[32] results in a straight line in which Δ_0 increases with increasing a_0. This relationship is supported by high-pressure measurements in Ge, for example, which show that $\Delta_0(P)$ is proportional to $a_0(P)^x$ where P is the hydrostatic pressure and $x\cong4$.[33] Similar relationships hold for all zinc-blende and diamond-structure semiconductors, but the exponent depends on the detailed structure of the valence band.[33] The scatter in Δ_0 values in the Δ_0 vs a_0 plot (where Δ_0 ranges from 10 to 803 meV) about a least-squares fit to the data is ±0.26. Inserting β-GaN, with $a_0=0.4530$ nm (Ref. 3) into this plot yields a value of 15.4±10 meV. Thus, our experimentally determined Δ_0 value for β-GaN is well within the scatter in the empirical relationship.

Figure 5 shows typical PL spectra at temperatures between 10 and 140 K from a β-GaN sample grown by RIMBE at $T_s=650\,°C$. In the low-temperature spectra, $T\leq20$ K, there are three spectral features present. At $T=10$ K, the strongest PL peak is observed at 3.291 eV, very close in energy to that of the fundamental band gap, E_0 (10 K)=3.302 eV from Fig. 2. A smaller peak is also present at 3.173 eV with a weak emission band at 3.49 eV. The energy position of the 10 K near-gap peak at 3.291 eV decreases in parallel to that of $E_0(T)$ with increasing T until it disappears at temperatures above ≅140 K. The width and shape of the peak indicate that it may be composed of two emission bands. Since all the films are *n*-type, the most common centers at low temperatures are expected to be neutral donors. Thus, we believe that one or both components of this peak correspond to radiative recombination from a very shallow

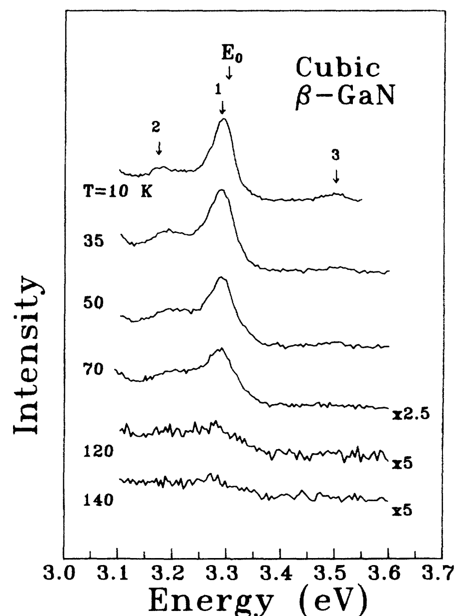

FIG. 5. Photoluminescence spectra from zinc-blende structure β-GaN at temperatures between 10 and 140 K.

donor level to the valence band. The fact that the energy difference between this peak and E_0 remains constant with T provides support for this interpretation since the shallow donor level and the conduction-band edge should shift in parallel. Emission from this band is quenched at temperatures above 100 K due to thermal ionization of the donor states.

The broad PL band centered at 3.173 eV at 10 K, approximately 130 meV less than the band-gap energy, is of weak intensity and is no longer visible above 80 K. With increasing temperature, it broadens further and the peak position shifts to higher energies. At 50 K, where the peak is still clearly observable, it is centered at 3.197 eV. Based upon its characteristic behavior, we tentatively assign this peak to a donor-acceptor pair recombination transition.[34]

The 10 K emission band at 3.49 eV is well above the fundamental band gap of α-GaN as determined from the PR results presented above, but close to reported values, 3.503 eV at 2 K,[35] for the wurtzite-structure α-GaN phase. Powell *et al.* note in Ref. 3 that some of the present samples exhibit small regions of α-GaN, which nucleate in the bulk and are entirely surrounded by the zinc-blende structure β-GaN. Based upon x-ray diffraction (XRD) measurements, they estimated that the maximum volume fraction is always less than 10^{-3}. We suggest that previously reported high-energy CL bands, which were originally assigned to band-to-band recombination from β-GaN, such as the feature which varied from 3.52 eV at 4 K to 3.45 eV at 300 K reported by Strite *et al.*[6] are in fact due to α-GaN inclusions.

Finally, we would like to point out that there are not strain effects, due either to lattice misfit or to the difference in thermal expansion coefficients between the GaN films and the MgO substrates, on the β-GaN E_0 and $E_0+\Delta_0$ energies reported in this paper. XRD and electron diffraction measurements show that the films are relaxed,[3] as expected due to both the large 7.5% compressive lattice misfit and also the large 59% differential thermal contraction stress. TEM and XTEM (Ref. 3) shows the formation of dislocations and stacking faults with the defect density being extremely high within about 100 nm of the film and/or substrate interface and much less at higher thickness. To avoid seeing effects due to strain in the reflectivity measurements, we used samples 1–1.5 μm thick. There are similar very large misfits and thermal stresses on the other substrates that have been used for growing β-GaN, such as GaAs and Si. Thus, one expects that films grown on these other types of substrates will also be relaxed, and hence, the optical parameters determined in this work applies to β-GaN samples grown on different substrates, as long as they are thick enough to be totally relaxed.

IV. CONCLUSIONS

We have used modulated photoreflectance measurements to make temperature-dependent measurements of the direct optical band gap E_0 (3.302 eV at 10 K to 3.231 eV at 300 K) and the valence-band spin-orbit splitting Δ_0 in metastable zinc-blende structure β-GaN. The temperature dependencies of both E_0 and $E_0+\Delta_0$ were well described by the empirical Varshni relationship, which has previously been shown to hold for a wide range of cubic semiconductors. The position of the spin-orbit split band at the center of the Brillouin zone was determined to be 17 meV below the fourfold degenerate valence band. The dominant low-temperature photoluminescence peak, which occurred at 11 meV below the conduction-band edge was attributed to a transition between a shallow donor level and the valence band.

ACKNOWLEDGMENTS

The authors gratefully acknowledge the financial support of Consejo Nacional de Ciencia y Tecnología, México through Grant No. 0444-E9108, the Organization of American States, Secretaría de Educación Pública, the Materials Science Division of the U.S. Department of Energy under Contract No. DEAC0276ER01198, the Joint Services Electronic Program, and the Semiconductor Research Corporation during the course of this research. We also appreciate the technical support of E. Ontiveros and L. F. Lastras-Martínez.

APPENDIX

The electroreflectance low-field limit is defined by the relationship[17]

$$\hbar\Omega \le \Gamma/3 , \tag{A1}$$

where the electro-optical energy $\hbar\Omega$ is given by

$$\hbar\Omega = \left[\frac{eF\hbar}{\delta\mu_{\parallel}} \right]^{1/3} . \tag{A2}$$

In Eq. (A2), F is the surface electric field and $\mu_{\parallel}=m_c m_v/(m_c+m_v)$ is the interband reduced mass, where m_c and m_v correspond to the conduction- and valence-band masses, respectively, evaluated in the field direction for the transition of interest. We estimate that $F=100$ kV cm^{-1}, and $\mu_{\parallel}$ is between 0.1 and 0.01 of the free electron mass. Using these values in Eq. (A2), $\hbar\Omega \cong 6-13$ meV, which is comparable to our experimental values of $\Gamma/3 \cong 3-7$ meV. Thus, we estimate that our PR data were obtained under conditions that correspond to being near or just above the low-field limit. Nevertheless, since the energy positions of the actual transitions are primarily determined by the "center of mass" of the PR modulated signal, the analysis of the results is not strongly sensitive to the precise details of the model used. This has been shown explicitly by Aspnes and Rowe[19] for the E_0 direct gap of Ge. The same E_0 value, within 2 meV, was obtained from fitting two experimental spectra, one corresponding to low-field conditions (0.6 kV cm^{-1}) and the other to high-field conditions (31 keV cm^{-1}), even though the two spectra exhibited quite different line shapes.

*Present address: Solar Cells Inc., 1702 N. Westwood Ave., Toledo, Ohio 43607.

[1]H. P. Maruska and J. J. Tietjen, Appl. Phys. Lett. **15**, 327 (1969).
[2]K. Das and D. K. Ferry, Solid-State Electron. **19**, 851 (1976).
[3]R. C. Powell, N. E. Lee, Y. W. Kim, and J. E. Greene, J. Appl. Phys. **73**, 189 (1993).
[4]R. C. Powell, G. A. Tomasch, Y. W. Kim, J. A. Thornton, and J. E. Greene, in *Diamond, Silicon Carbides and Related Wide Bandgap Semiconductors,* edited by J. T. Glass, R. F. Messier, and N. Fujimori, MRS Symposia Proceedings No. 162 (Materials Research Society, Pittsburgh, 1990), p. 531.
[5]M. Mizuta, S. Fujieda, Y. Matsumoto, and T. Kawamura, Jpn. J. Appl. Phys. **25**, L945 (1986).
[6]S. Strite, J. Raun, Z. Li, A. Salvador, H. Chen, D. J. Smith, W. J. Choyke, and H. Morkog, J. Vac. Sci. Technol. B **9**, 1924 (1991).
[7]M. J. Paisley, Z. Sitar, C. H. Carter, and R. F. Davis, Proc. SPIE **877**, 8 (1988).
[8]M. J. Paisley, Z. Sitar, J. B. Posthill, and R. F. Davis, J. Vac. Sci. Technol. A **7**, 701 (1989).
[9]T. Lei, M. Fanciulli, R. J. Molnar, T. D. Moustakas, R. J. Graham, and J. Scanlon, Appl. Phys. Lett. **59**, 944 (1991).
[10]S. Bloom, G. Harbeke, E. Meier, and I. Ortenburger, Phys. Status Solidi B **66**, 166 (1974).
[11]B. J. Min, C. T. Chan, and K. M. Ho, Phys. Rev. B **45**, 1159 (1992).
[12]W. R. Lambrecht and B. Segall (unpublished).
[13]K. Okumura, S. Misawa, and S. Yoshida, Appl. Phys. Lett. **59**, 1058 (1991).
[14]R. F. David, Proc. IEEE **79**, 702 (1991).
[15]R. E. Nahory and J. L. Shay, Phys. Rev. Lett. **25**, 290 (1970).
[16]D. E. Aspnes and A. A. Studna, Phys. Rev. B **7**, 4605 (1973).
[17]D. E. Aspnes, Surf. Sci. **37**, 418 (1973); see also, D. E. Aspnes in *Optical Properties of Solids,* edited by M. Balkanski (North-Holland, Amsterdam, 1980), Vol. 2, p. 109.
[18]F. Bassani and G. P. Parravicini, *Electronic State and Optical Transitions in Solids,* edited by R. A. Ballinger (Pergamon, London, 1975), Chap. 3, p. 67, and Chap. 5, p. 149.
[19]D. E. Aspnes and J. E. Rowe, Phys. Rev. Lett. **27**, 188 (1971).
[20]Y. P. Varshni, Physica **34**, 149 (1967).
[21]E. Edjer, Phys. Status Solidi A **6**, K39 (1971).
[22]D. E. Aspnes, C. G. Olson, and D. W. Lynch, Phys. Rev. B **12**, 2527 (1975).
[23]J. Camasel, P. Merle, L. Bayo, and H. Mathien, Phys. Rev. B **22**, 2020 (1980).
[24]A. Onton, in *Proceedings of the Tenth International Conference on Physical Semiconductors,* Cambridge, MA, 1970 (USAEC, New York, 1970), p. 107.
[25]F. Lukes, Phys. Status Solidi B **84**, K113 (1977).
[26]D. E. Aspnes, C. G. Olson, and D. W. Lynch, Phys. Rev. B **14**, 4450 (1976).
[27]K. C. Rustagi, P. Merle, D. Auvergne, and H. Mathien, Solid State Commun. **18**, 1201 (1976).
[28]R. L. Aggarwal, in *Semiconductors and Semimetals,* edited by R. K. Williardson and A. C. Beer (Academic, New York, 1972), Vol. 9, p. 151.
[29]D. E. Aspnes and A. A. Studna, Solid State Commun. **11**, 1375 (1972).
[30]D. E. Aspnes, Phys. Rev. B **12**, 2297 (1975).
[31]S. H. Groves, E. R. Pidgeon, A. W. Ewald, and R. J. Wagner, J. Phys. Chem. Solids **31**, 303 (1970).
[32]R. G. Humphreys, D. Bimberg, and W. J. Choyke, J. Phys. Soc. Jpn. **49**, 519 (1980).
[33]D. Brust and L. Liu, Solid State Commun. **4**, 193 (1966).
[34]F. Williams, Phys. Status Solidi **25**, 493 (1968).
[35]B. Monemar, Phys. Rev. B **10**, 676 (1974).